

Higher-dimensional approach to a unified growth model for crystals, quasicrystals, and multiply twinned particles

J. L. Aragón, D. Romeu, and A. Gómez

Instituto De Fisica, Universidad Nacional Autonoma de Mexico, Apartado Postal 20-364, México D. F., 01000, Mexico

(Received 30 August 1990; revised manuscript received 17 December 1990)

In this work the decahedral-recursive (DR) growth model, which generates both crystals and quasicrystals of all symmetries, is formulated in the context of the cut-projection method. In this approach all operations in the higher-dimensional space are justified by physical laws in three dimensions. Although all competing geometrical models of quasicrystals can be formulated in this language, the most physically significant equilibrium structures are found to be those from the so-called random tiling. The similarities and differences between DR and other schema are presented and analyzed.

I. INTRODUCTION

A lively debate¹⁻⁴ has existed over choosing a theoretical model that attempts to explain the structural properties of quasicrystals, since their discovery in 1984.⁵ Existing models fall into three main classes: the “perfect quasicrystal” (PQ), based on Penrose-like tilings,⁶⁻⁸ the “random quasicrystal” (RQ), based on random packing of tiles such as Amman rhombohedra,⁹⁻¹² and the “icosahedral glass” (IG), based on random packings of icosahedral clusters.^{13,14}

More recently, a nucleation and growth approach to the problem led to the atomistic decahedral-recursive (DR) model.¹⁵⁻¹⁸ The DR model regards growth as a two-stage process. The first (decahedral growth) describes how atoms in the liquid add to the solid-liquid interface to form clusters. The second stage (recursive growth) describes (still following stage-1 rules) how clusters aggregate to form a macroscopic structure. In this way the model explains the formation of clusters that other models use as a starting point. But most importantly, the growth rules are derived from well-established physical principles instead of “guessed” from analysis of particular known structures and are therefore the same for all metals. This gives the model a sound physical foundation and great generality, allowing it to describe the growth and basic structure of crystals, multiply twinned particles, and quasicrystals of various symmetries such as icosahedral (I), decagonal (T),^{15,16} octagonal, and dodecagonal.¹⁸ Also, it predicts the existence of additional possible phases.¹⁷

The purpose of this paper is to present a higher-dimensional approach to the DR model. In this approach, the model is viewed as a projection onto three-dimensional (3D) space of a subset of points of a hyperlattice including a well-defined decoration. This allows the DR model to be phrased in a more common (and powerful) language which permits the study long-range-order properties of the clusters and also compare and relate the DR to others. It will be shown that DR is a complete atomic structure model for quasicrystals, in the sense that it has adjustable parameters that can be optimized in fits

to experimental data and is capable of generating both tilings of rhombohedra and packings of icosahedral clusters.^{8,9,19}

The paper is outlined as follows. After briefly reviewing the quoted models in Sec. II, focusing on their higher-dimensional representations, Sec. III describes the higher-dimensional approach to the DR model and some of its consequences, Sec. IV presents the diffraction properties of the projected structures and, finally, in Sec. V we summarize and discuss the results.

II. QUASICRYSTAL MODELS

A. Structural classes

For comparison purposes, and leaving aside the decoration, existing quasicrystal structural models can be divided, according to the geometry of the framework, into three classes.²⁰

Class I: Perfect Quasicrystal. The distinctive feature of models in this class is that the resulting structures are quasiperiodic. Here, the framework is built by repeated use of fundamental units (tiles), which are almost always taken to be the Amman rhombohedra,^{21,22} and is completely deterministic in its construction. An example is the Penrose tiling consisting in Amman rhombohedra plus matching rules.⁶⁻⁸

Class II: Random Tiling. Also constructed by using elementary tiles but matching rules are now violated at some places. The unique restriction is that neighboring vertices are linked together by bonds along symmetry directions occurring with equal frequency.^{9-12,19}

Class III: Icosahedral Glass. This is a random structure built with the sole restriction of minimum distance between vertices without the restriction of Class II, i.e., there are vertices which are not properly linked.^{13,14}

B. Higher-dimensional representation

It is convenient and useful to represent the structures discussed in Sec. IIA as obtained by the projection of a set of points of a periodic lattice \mathcal{Q} , in a higher N -dimensional space, onto an n -dimensional appropriately

oriented hyperplane E'' (the real space). In the three cases discussed above the set of lattice points must project onto the vertices of the framework which, in a decorated model, must correspond either to an atom or to a cluster center.^{9,10,19} The set of projected points can be parametrized as follows.

Given a structure in n dimensions, it is always possible²³ to find an N -dimensional lattice \mathcal{L} with basis $\{\mathbf{e}_i\}_{i=1}^N$, such that each vertex of the structure is the projection, onto E'' , of a point

$$\mathbf{r} = \sum_{i=1}^N n_i \mathbf{e}_i \quad (1)$$

with integers n_i . It is useful to decompose the vectors \mathbf{r} into components \mathbf{r}'' , lying in the physical n -dimensional E'' space, and a $(N-n)$ -dimensional \mathbf{r}^\perp vector lying in E^\perp , the orthogonal complement to E'' . The vertices in \mathbf{R}^N then form a lattice with coordinates (n_1, n_2, \dots, n_N) generated by $\{\mathbf{e}_i\}_{i=1}^N$. The sum $\mathbf{r}'' + \mathbf{r}^\perp$ describes the same vertex but in projected coordinates $(\mathbf{e}_i'', \mathbf{e}_i^\perp)$.

Because vertices in physical space correspond to atoms or cluster centers, a nonoverlap condition must be imposed, forcing the map from E'' to \mathcal{L} , and consequently, from E'' to E^\perp , to be one-to-one. Therefore, the function $\mathbf{r}^\perp(\mathbf{r}'')$ is single valued and defines a hypersurface in \mathbf{R}^N . This hypersurface contains all the available information about symmetry and diffraction properties of the projected structure. A PQ (class I) corresponds to $\mathbf{r}^\perp \approx \text{const}$, so that the embedded hypersurface approximates E'' as closely as possible. A RQ (class II) corresponds to a rippled but unbroken hypersurface, while in class II the defects (forbidden links) give rise to hypersurface tears, across which \mathbf{r}^\perp changes discontinuously.²⁰

In the cut-projection (strip) formalism,²⁴⁻²⁶ the set of points of \mathcal{L} to be projected must lie inside a "strip" as illustrated in Fig. 1. The "shape" of this strip constitutes the difference between existing models. A perfect quasicrystal is obtained with a straight strip obtained by translating the unit cell of the lattice along a line parallel to E'' as shown in Fig. 1. Deviations of the strip slope from the E'' orientation lead to deviations from

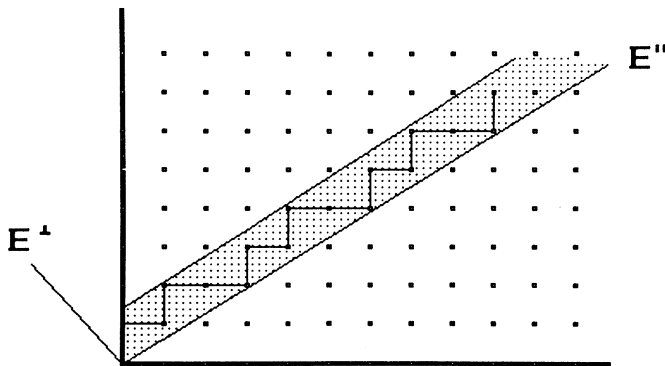


FIG. 1. Two-dimensional example of the cut-projection method. The points inside the strip (dashed) are projected onto E'' .

icosahedral orientational symmetry. If the inclination of the strip is allowed to fluctuate while maintaining the correct slope in average (a rippled but unbroken strip), the projected structure may preserve long-range orientational symmetry and will still be constructed with rhombuses, but matching rules will be violated. This is the RQ model, where, depending on the severity of the fluctuations, the structure may maintain long-range or quasi-long-range translation order. The extreme case, when the strip is permitted to have breaks, corresponds to the IG model; in this case, orientational symmetry may be preserved⁹ but the resulting tiling will not fill space and, although the system may have long correlation lengths, they will generally be finite.

III. DECAHEDRAL-RECURSIVE MODEL

A. Summary

The decahedral growth stage of the model is based on the observation that the most stable magic number particles²⁷⁻³⁰ are composed of a complete number of irregular decahedra (pentagonal bipyramids). The model assumes that growth completing decahedra constitutes a minimum energy path,^{17,27} so that atoms in the liquid tend to be added to the solid phase completing interpenetrating decahedra. This is so because in this way atoms complete more than one (irregular) tetrahedron simultaneously and tetrahedral packing is highly efficient. This is actually realistic since we know that for small clusters of atoms as in the initial stages of crystallization, the magic numbers (i.e., 13) minimize the surface energy of the cluster. Therefore, the model assumes that embryos with magic number structure are present in the liquid as heterophase transitions acting as nucleation sites. Decahedral growth is then applied to the various magic numbers, the first two (13 and 19) giving rise to the I and T phases, respectively, and the others giving rise to other phases.

The recursive stage of the model is based on the results of the coincidence site lattice model^{31,32} (CSL) which predicts the existence of a low energy (good atomic fit) boundary between crystals oriented so that their infinite lattices have a subset of coinciding points. The higher the percentage of coincidences, the lower the elastic energy, so one expects a higher probability for growth of properly oriented grains at these sites.

It is observed that when DR structures are shifted into the positions of some of their own atoms, a large number of coincidences between original and shifted atoms result. The recursive stage of the model then consists of taking clones of a given DR structure and bringing them into these high coincidence origins (discarding atoms in the intersection volume). This gives rise to a larger stable structure which, according to the CSL should have a low energy cluster-cluster interface. Remarkably, the model works so well that such interfaces are not only low energy but coherent (indistinguishable under the electron microscope).¹⁷ In this sense, these atoms have the property of being "good origins" and are referred to as O atoms or O points. The process is then repeated recursively produc-

ing structures with local bond orientational order, sharp diffraction peaks, and mechanical stability (near a local minimum) under a Lennard Jones interaction, meaning volume is efficiently filled.

The physics behind this stage is very simple. It turns out that O atoms are always located at positions in the solid-liquid interface that are centers of partially completed and slightly distorted icosahedra (Fig. 2), having also the important geometrical property of being expressible as integral combinations of an icosahedral star. Therefore, there is a lowering of energy when the atoms in the liquid complete these icosahedra restarting the growth process again using the selected O point as a new origin. From this point of view, the full growth process proceeds by completing decahedra (stage 1), constantly yielding new possible centers (O points) which the system may (stage 2) or may not use as new origins, depending on external conditions.

Although the DR model is based on growth through a minimum (internal) energy path, it can lead (using additional entropy-maximizing hypothesis) to structures where the free, rather than just the internal energy is also minimized, explaining equilibrium quasicrystals (see Sec. III C 2). In this case, the growth path becomes of secondary importance although it must be remembered that equilibrium phases also form through nucleation and growth.

The above results are valid in general. However, for comparison purposes we will confine ourselves to the quasicrystalline I phase for which other theories have been extensively developed.

DR structures are composed of "shells" of atoms with the same distance to the origin, consisting of polyhedra with the symmetry of the initial seed. It is convenient to use the smallest possible subset of atoms from a given DR structure that can give rise to a quasicrystal by the shift

and add mechanism outlined above. The three first shells of the first DR cluster produced¹⁵ meet this condition. They are a unit icosahedron (the seed) hereafter referred to as ICO1, a dodecahedron (DODE) with atoms sitting on the faces of ICO1, and a second icosahedron (ICO2) with circumradius twice that of ICO1. Note that the star ICO1-DODE-ICO2 describes well the Al-Cu-Li-type alloys whereas the aluminum-transition-metal alloys require the star composed of the first three shells of a Mackay icosahedron: ICO1-ICOSIDODECAHEDRON-ICO2. Both stars are, however, obtainable from the DR model since both are composed of a complete number of interpenetrated decahedra (Fig. 3). The Mackay star is produced by shifting ICO1 star into its own surface atoms.

In the case of the ICO1-DODE-ICO2 star, the atoms of the ICO2 shell and its integral combinations [see Eq. (2)] satisfy the O point conditions and the set of O atoms form a substructure expressible as integral combinations of ICO2.¹⁷ So, if $\{\mathbf{a}_i\}_{i=1}^6$ is the (unit) icosahedral star, the substructure \mathcal{O} of O points is given by

$$\mathcal{O} = \left\{ o_j = \sum_{i=1}^6 n_i \mathbf{a}_i \text{ for some } n_i | n_i = 0, \pm 2, \pm 4, \dots \right\}. \quad (2)$$

The set \mathcal{O} forms a skeleton which may or may not be quasiperiodic and will play an essential role in what follows.

Summarizing, the recursive stage consists of the following steps:¹⁷

1. A *Basic Star* $\{\mathbf{b}_i\}_{i=1}^r$ is chosen (in this case, the ICO1, DODE, and ICO2 star, i.e., $r=44$).
2. This star is shifted into the positions of a definite set of atoms, namely, the O atoms. First the star is shifted

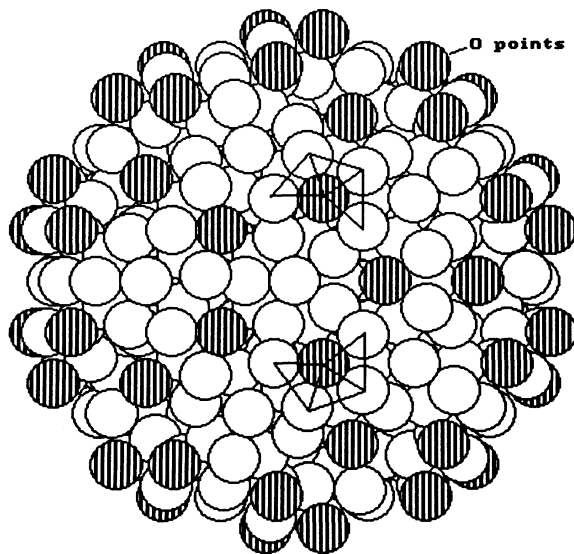


FIG. 2. Icosahedral cluster showing O points are at the centers of incomplete distorted icosahedra.

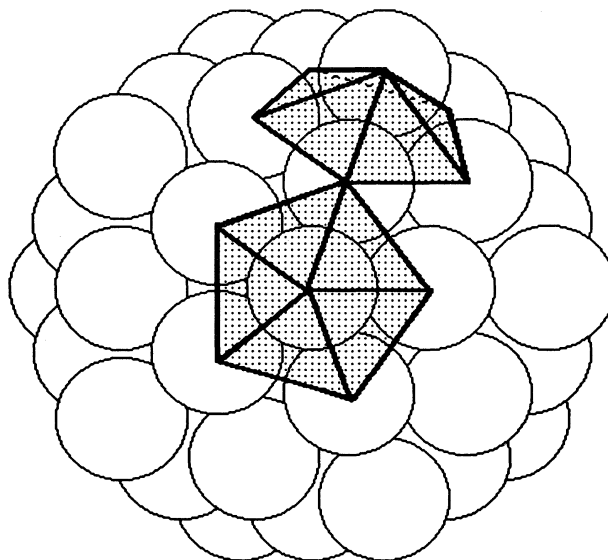


FIG. 3. The 55-atom Mackay icosahedron composed of a complete number of interpenetrated decahedra. Two decahedra are shown.

into the ICO2 set and in later steps into some of its integral combinations. As a result of this step, a number of coincidences are obtained but also noncoincident overlapping atoms.

3. Nonoverlapping atoms, i.e., those disting not less than 90% of the unit atomic diameter from others already present, are added to the structure and step 2 is repeated.

A higher-dimensional representation of the resulting structures is the objective of the next section.

B. Higher-dimensional representation

In a recent paper³³ we have shown that if a cut-projection method is applied in order to obtain icosahedral DR quasicrystals, we must consider a lattice $\mathcal{L} \subset \mathbf{R}^6$ of size 2 defined as

$$\mathcal{L} = \left\{ \mathbf{r} = \sum_{i=1}^6 n_i \mathbf{e}_i \mid n_i = 0, \pm 2, \pm 4, \dots \right\}, \quad (3)$$

where $\{\mathbf{e}_i\}_{i=1}^6$ is the canonical basis of \mathbf{R}^6 . The lattice must be decorated in such a way that the points \mathbf{r} project onto points of the ICO2 family (the O point skeleton) and the decoration onto ICO1 and DODE.

In this way, the decoration must lie at positions of the family $\{100\,000\}$ (the midpoints of the ICO2 vectors in \mathbf{R}^6) and $\frac{2}{3}\{111\,000\}$ (the 20 points that project into the vertices of DODE).

Given the lattice \mathcal{L} decorated as described, there is a straightforward way to generate a strip in order to produce the same DR structures of last section. The method consists in lifting the 3D substructure obtained after each step of the DR model as follows (see Fig. 4).

Let S_0 be a portion of strip called “basic slab” defined as the set

$$S_0 = \{ \mathbf{x} = (\mathbf{x}'', \mathbf{x}^\perp) \mid \mathbf{x}^\perp \in \Omega, x'' \leq 2 \}, \quad (4)$$

where the orthogonal decomposition $\mathbf{x} = (\mathbf{x}'', \mathbf{x}^\perp)$ has been used. Ω is the acceptance region obtained by projecting orthogonally the fundamental domain of the lattice (in this case, a hypercube of size 2), onto E^\perp , and x'' is the magnitude of the vector \mathbf{x}'' .

According to its definition, S_0 contains only those points of the decorated hyperlattice which project onto the basic star $\{\mathbf{b}_i\}_{i=1}^{44}$: the ICO1-DODE-ICO2 star. S_0 projects into E'' as a sphere of radius 2 containing the centers of the ICO1-DODE-ICO2 atoms.

By lifting the set \mathcal{O} defined in (2), it is easy to see that the O points in 3D correspond to lattice points in 6D, in such a way that an O point \mathbf{o}'' in 3D space lifts into a point $\mathbf{o} = (\mathbf{o}'' + \mathbf{o}^\perp) \in \mathcal{L}$. So, the next step consists in shifting the basic slab S_0 into the positions of a set of points $\mathbf{o}_i \in \mathcal{L}$ and the nonoverlapping requirement in 3D (Sec. III A) is equivalent to a first approximation, to a nonintersecting requirement of the projections onto E'' of neighboring slabs.

The fact that we are trying to model a “real” atomistic process, poses a difficulty not found in entirely geometrical models. In our case, points contained in the basic slab project into 3D as atoms having finite volume (unit

diameter for all atoms is assumed for simplicity). Therefore, in order to prevent overlapping, an extra 0.5 radius must be given to the 3D sphere [and to the already projected section of the strip in Eq. (6)] into which the basic slab has been projected so that it contains the full volume of its associated atoms. A simple calculation shows that no extra atoms can be placed inside such a sphere without overlap. Conversely, given that there is an O point at a distance of 2.0 or less from any given point in physical space, and that spheres around these can overlap, physical space can be completely covered by such spheres.

Accordingly, the initial step generates the strip segment

$$S_1 = S_0 \cup (S_0 + \mathbf{o}_1) - \{ \mathbf{x}' \in (S_0 + \mathbf{o}_1) \mid P''(\mathbf{x}') \in P''(S_0) \}, \quad (5)$$

where \mathbf{o}_1 (the first lifted O point) is one vertex of the hypercube and P'' denotes the orthogonal projector onto E'' , so that, the subtracted set is the portion containing points that would project onto “occupied volume” in 3D.

The j th step then gives

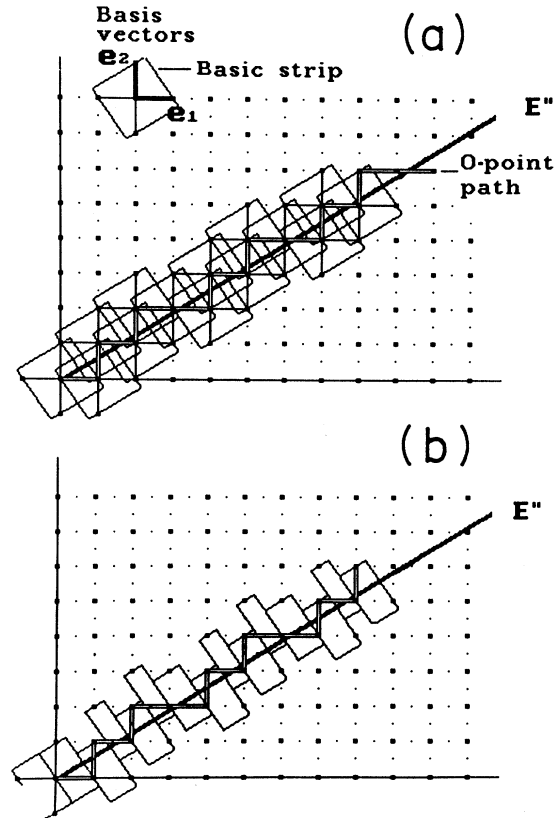


FIG. 4. Two-dimensional example of the strip construction following the procedure described in the text to obtain a DR structure. (a) The basic strip or basic slab S_0 is translated onto the points of a Fibonacci staircase (O point path). (b) Final aspect of the strip after discarding overlapping.

$$S_j = S_{j-1} \cup (S_0 + \mathbf{o}_j) - \{\mathbf{x}' \in (S_0 + \mathbf{o}_j) | P''(\mathbf{x}') \in P''(S_{j-1})\}, \quad (6)$$

where $\mathbf{o}_j \in \mathcal{L}$ is in the set of lifted O points. By this procedure we can generate an infinite staircaselike strip simply shifting S_0 into the positions of all the lifted O points and discarding in each step, the section of S_0 overlapping the existing strip. According to the discussion above, the overlap test is done against the existing strip assuming it has an extra E'' width of 0.5 in order to properly model the “real” 3D behavior. Note, however, that this does not alter the shape of the strip so that diffraction properties are not affected (see Sec. IV). Figure 4 shows the strip in the trivial 2D case for a particular selection of O points. The O point selection criterion is discussed in the following sections. In order to complete the analogy with the icosahedral case, a cubic lattice with decoration at the midedges simulating ICO1 is also shown (DODE cannot be drawn in 2D).

Note that the resulting strip consists of the union of disjoint slabs S_i having different width in E'' so that an alternative definition of the strip S can be

$$S = \bigcup_{i=1}^{\infty} S_i \quad \text{and} \quad P''(S_i) \cap P''(S_j) = \emptyset \quad \text{for} \quad i \neq j. \quad (7)$$

The important point to notice here is that two different sections S_i (with equal E^\perp but different E'' widths), are related by a shift through the perpendicular component of a lattice point. For example, the portion S_i is related to S_{i-1} by a shift \mathbf{o}_i^\perp , where $\mathbf{o}_i (= \mathbf{o}_i'' + \mathbf{o}_i^\perp) \in \mathcal{L}$ (Fig. 4).

A comment about the uniqueness of the resulting structures is granted here. It turns out that the local surroundings around O points belonging to the same orbit of the icosahedral group are the same when the orbits are “filled” in an orderly manner, i.e., one orbit at a time, in accordance with a given rule, which could be filling first orbits with minimum E^\perp component or maximum number of coincidences. In other words, the order in which atoms are filled within a given orbit is immaterial. This is not necessarily true when atoms from different orbits are filled at random. This means that given a staircase of O points, the structure is unique proved O points are filled orbit by orbit.

C. Geometry of the clusters

For the sake of comparison with other models, it is useful to adopt the approach discussed in Sec. II B of considering the fluctuations of the orientation of the strip around the average orientation. According to last section, it is easy to see that the average slope and roughness (fluctuations around the average slope) of the hypersurface defined by the hyperlattice points within the strip, depend on the choice of O points at each step, or the “path” the system follows during growth. Note that this path can be optimized in order to fit the experimental data. This section shows how with an adequate selection of the growth path, we can obtain structures with different framework geometries, as a matter of fact, it is

possible to obtain the most popular ones: tilings of rhombohedra and packings of icosahedral clusters.

1. Rhombohedral tilings

When the strip is built as described in Sec. III B all O points are linked by bonds of proper orientation, so the strip is rippled but unbroken, leading to real-space structures with a framework that can be viewed as packings of a well-defined set of tiles.

A simple example can serve to illustrate this point. In order to ensure long-range translational order, a natural way to generate the hypersurface (growth path) is to choose the O points (hyperlattice points) in such way that it approximates E'' as closely as possible; this means selecting at each step, only those O points having minimal phason (i.e., E^\perp) component thus producing an hypersurface with the smallest possible deviation from irrational slope. Starting with the ICO1-DODE-ICO2 basic star we can generate a nonperiodic structure by recursive application of this star upon a selected set of points, as described in Sec. III A. At first there are only 12 O points (the ICO2) all having the same phason component, so the basic star is shifted into these positions. In the following steps, only the set of minimal phason component O points are selected as good O points.

The first stages of the O point skeleton growth in this case are illustrated in Fig. 5. After the first three itera-

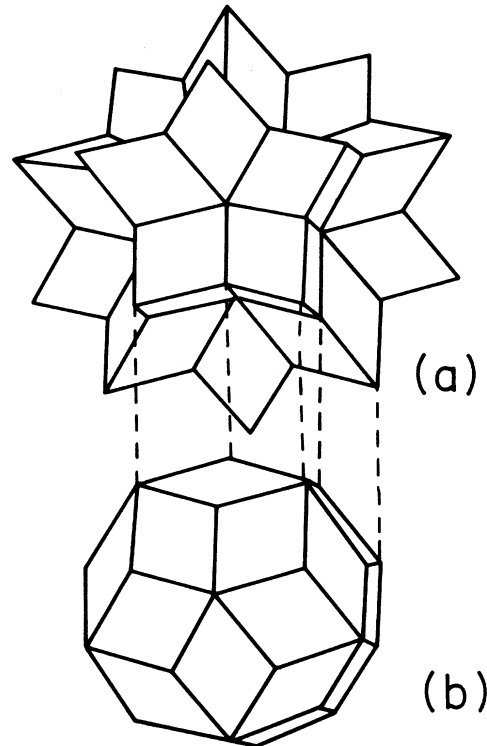


FIG. 5. First stages of the O point skeleton growth. (a) O point skeleton after three iterations defining a central stellation composed of 20 prolate rhombohedra. (b) One of the 12 rhombic triacontahedra formed along the fivefold axes of the central stellation after four more iterations.

tions, a central stellation, formed from 20 prolate rhombohedra [Fig. 5(a)], is obtained. The next four iterations give a centrosymmetrical framework which can be viewed as a cluster of 12 rhombic triacontahedra placed along the fivefold axes of the central stellation. One of these triacontahedra is shown in Fig. 5. At this stage, the framework is identical to that proposed in Ref. 34 based on a topologically disordered icosahedral quasilattice and proposed as a model for the Al-Mn-Si phase. Notable differences with this model develop at later stages.³⁵

In this example, all O points with minimal phason component are filled at each step; different configurations of this kind of tiling are obtained when the selection criterion is varied. For instance, using a given subset of minimal O points (see next section).

It is important to note that the DR model is an atomistic model, so it produces decorated structures. In the precedent case, for instance, the framework is defined by the set of O points and the decoration by the ICO1 and DODE substars.³³ The important point which establishes a major difference with other structural models, is that there is not a unique decoration for each tile in real space. Instead, the present model proposes an identical decoration of the higher-dimensional hyperlattice points, so that 3D tiles are not necessarily decorated identically. Note that if attention is restricted to the O points (neglecting decoration) the projected structure is a conventional tiling. But if the decoration of the higher-dimensional lattice is included, the model cannot be seen as a pure tiling in which the tiles are either identically decorated or decorated with a small number of motifs. In this sense it is not a tiling model, though there is a tiling associated with it.

2. Cluster-based quasicrystal

In the example above, all O points with minimal phason component are "filled" at each step, since there are always O points available within a straight strip, this leads to a structure equivalent to the PQ models.

If one imposes the more physical condition that the number of coincidences must be maximized (internal energy minimized), one can generate important cluster-based structures. In particular, periodic networks isostructural with the $(\text{Al-Zn})_{49}\text{Mg}_{32}$ (Ref. 36) and $R\text{-Al}_5\text{Cu-Li}_3$ (Ref. 37) crystalline alloys which are, in fact, approximant structures for the Al-Zn-Mg class quasicrystal.^{38,39}

During the recursive process the first (having both minimal phason component and maximum coincidence sites) families (orbits) filled are sequentially: the $(000\ 000)$ origin, the $\{200\ 000\}$ icosahedron, the $\{220\ 000\}$ icosidodecahedron, and the $\{222\ 000\}$ dodecahedron. The vectors of the last $\{222\ 000\}$ family are parallel to the DODE vectors $\frac{2}{3}\{111\ 000\}$ pointing along threefold axes having the important property, besides minimal phason component, of giving rise to the maximum percentage of coincident sites.⁴⁰ This is because these points can be expressed as integral combinations of both ICO2 and DODE substar vectors. In terms of the CSL model, this

means that energy is reduced (coincidences increased) when the system chooses a growth path along the threefold axes. A tendency to grow along threefold axes is experimentally observed.⁴¹

Another important result is that the sequence of shells around $\{222\ 000\}$ points is the same that at the origin: ICO1-DODE-ICO2. In other words, the initial star (cluster) is recovered. If one chooses among the 20 available $\{222\ 000\}$ points to fill, only those oriented along the eight diagonals of a cube with origin at the center of the basic star, a cubic structure results in which the basic star is recovered completely at the vertices of the cube (points $\{222\ 000\}$) with the same orientation. The atomic positions of the resulting BCC packing of clusters is the same as the reported for the $(\text{Al-Zn})_{49}\text{Mg}_{32}$ crystalline alloy.³⁶ Details of these approximant structures as well as those based on Mackay clusters are given elsewhere.⁴⁰ In spite of the fact that in the DR model the overlap of icosahedral motifs is permitted, there exist O points paths that recover the initial icosahedral motifs at certain places, making it possible to generate cluster-based structures including a well-defined decoration and the so-called "glue" atoms which now appear naturally as part of the growth process.

A decorated random tiling network is produced by filling the $\{222\ 000\}$ points with equal probability. The RT model explains equilibrium quasicrystals assuming that free energy is minimized mainly through the entropy term when the $\{222\ 000\}$ points are filled with equal probability. Note that the DR model focuses its attention on a minimum internal energy path finding minimum energy clusters and a way to minimize interfacial cluster-cluster energy by joining them along threefold directions. No mention is made of the entropy term. However, the precise way in which clusters are joined can be chosen freely in the model so that the RT hypothesis of equal probability for each threefold direction can be adopted thus yielding RT structures.

So DR has potentially the advantages of the RT model but having access to the internal energy it does not need to postulate the existence of the clusters which in DR, are inferred from first principles. Thus, assuming the important internal energy terms are the cluster energy and the interfacial cluster-cluster energy and that the dominant entropy term is determined by the cluster packing, we are able to produce structures with minimal internal energy and maximum entropy. Note that here terms like the mixing entropy within clusters is ignored.

IV. DIFFRACTION

Given the higher-dimensional space formulation of the DR model, the general nature of the diffraction pattern can be specified easily. The approach followed is similar to that used in the cut-projection schema,²⁴⁻²⁶ the differences being (1) in DR the "band" has a complex shape with ups and downs according to the O points and (2) the hyperlattice itself is decorated.

In the following subsections the general diffraction expressions are derived.

A. General

The "mass density" of the lattice $\mathcal{L} \subset \mathbf{R}^N$ is given by

$$\rho_1(\mathbf{r}) = \sum_{\mathbf{l} \in \mathcal{L}} \delta(\mathbf{r} - \mathbf{l}) \quad (8)$$

with $\mathbf{r} \in \mathbf{R}^N$. If ρ_0 is the density of the "decoration" associated with each lattice point, and if ρ_2 is the density of the decorated lattice:

$$\rho_2(\mathbf{r}) = \rho_1(\mathbf{r}) * \rho_0(\mathbf{r}) = \sum_{\mathbf{l} \in \mathcal{L}} \rho_0(\mathbf{r}) * \delta(\mathbf{r} - \mathbf{l}) = \sum_{\mathbf{l} \in \mathcal{L}} \rho_0(\mathbf{r} - \mathbf{l}). \quad (9)$$

Let $W(\mathbf{r})$ be the "cut" function in \mathbf{R}^N defined by

$$W(\mathbf{r}) = \begin{cases} 1 & \text{if } \mathbf{r} \in S, \\ 0 & \text{if } \mathbf{r} \notin S, \end{cases} \quad (10)$$

where S is the given strip $S \subset \mathbf{R}^N$. The density of the cut crystal is, then,

$$\rho_3(\mathbf{r}) = \rho_2(\mathbf{r}) W(\mathbf{r}) = [\rho_1(\mathbf{r}) * \rho_0(\mathbf{r})] W(\mathbf{r}). \quad (11)$$

The projection of $\rho_3(\mathbf{r})$ along E^\perp is given by $\rho_4(\mathbf{r}'')$, where

$$\rho_4(\mathbf{r}'') = \int \rho_3(\mathbf{r}'', \mathbf{r}^\perp) d\mathbf{x}_1^\perp d\mathbf{x}_2^\perp \cdots d\mathbf{x}_{N-n}^\perp. \quad (12)$$

B. Fourier transforms

Using the section-projection theorem of Fourier transform theory, we have of the transform of ρ_4 the expression

$$\hat{\rho}_4(\mathbf{u}'') = \hat{\rho}_3(\mathbf{u}'', 0) \quad (13)$$

(here \mathbf{u} is written as $\mathbf{u} = \mathbf{u}'' + \mathbf{u}^\perp$, with $\mathbf{u}'' \in E''$ and $\mathbf{u}^\perp \in E^\perp$). But, from Eq. (11),

$$\hat{\rho}_3(\mathbf{u}) = \hat{W}(\mathbf{u}) * [\hat{\rho}_1(\mathbf{u}) \hat{\rho}_0(\mathbf{u})]. \quad (14)$$

Now from Eq. (8),

$$\hat{\rho}_1(\mathbf{u}) = \sum_{\mathbf{l} \in \mathcal{L}} \exp(-2\pi i \mathbf{u} \cdot \mathbf{l}) = V^* \sum_{\mathbf{l} \in \mathcal{L}^*} \delta(\mathbf{u}^* - \mathbf{l}). \quad (15)$$

Here, $\mathcal{L}^* \subset \mathbf{R}^N$ denotes the reciprocal lattice defined by

$$\mathcal{L}^* = \left\{ \mathbf{u}^* = \sum_{i=1}^N n_i \mathbf{a}_i^* \mid n_i \in \mathbf{Z} \right\}, \quad (16)$$

and where the $\{\mathbf{a}_i^*\}$ are defined, in turn, by

$$\mathbf{a}_i \cdot \mathbf{a}_j^* = \delta_{i,j}. \quad (17)$$

$$\hat{\rho}_4(\mathbf{u}'') = V^* \sum_{\mathbf{l} \in \mathcal{L}^*} \sum_{i=1}^k \hat{\rho}_i^3(\mathbf{l}^{*''}) \exp(-2\pi i \mathbf{l}^{*''} \cdot \mathbf{r}_i) \hat{W}(\mathbf{u}'' - \mathbf{l}^{*''}, -\mathbf{l}^{*\perp}). \quad (26)$$

The choice given by Eqs. (23) and (24) is the simplest one giving, upon projection onto E'' , the ordinary atomic scattering factors.

D. General characteristics of the diffraction pattern

Equation (26) governs the nature of the diffraction patterns and several important cases can be singled out.

The quantity V^* is the reciprocal-space unit-cell volume. With these expressions we have

$$\hat{\rho}_1(\mathbf{u}) \hat{\rho}_0(\mathbf{u}) = V^* \sum_{\mathbf{l} \in \mathcal{L}^*} \hat{\rho}_0(\mathbf{l}^*) \delta(\mathbf{u} - \mathbf{l}^*) \quad (18)$$

and

$$\begin{aligned} \hat{\rho}_3(\mathbf{u}) &= V^* \left[\hat{W}(\mathbf{u}) * \sum_{\mathbf{l} \in \mathcal{L}^*} \hat{\rho}_0(\mathbf{l}^*) \delta(\mathbf{u} - \mathbf{l}^*) \right] \\ &= V^* \sum_{\mathbf{l} \in \mathcal{L}^*} \hat{\rho}_0(\mathbf{l}^*) W(\mathbf{u} - \mathbf{l}^*). \end{aligned} \quad (19)$$

If $\mathbf{l}^* = \mathbf{l}^{*''} + \mathbf{l}^{*\perp}$, with $\mathbf{l}^{*''} \in E''$ and $\mathbf{l}^{*\perp} \in E^\perp$, we obtain, finally,

$$\hat{\rho}_4(\mathbf{u}'') = V^* \sum_{\mathbf{l} \in \mathcal{L}^*} \hat{\rho}_0(\mathbf{l}^*) \hat{W}(\mathbf{u}'' - \mathbf{l}^{*''}, -\mathbf{l}^{*\perp}). \quad (20)$$

C. How to calculate $\rho_0(\mathbf{u})$

Let $\mathbf{r}_1, \mathbf{r}_2, \dots, \mathbf{r}_k$ ($k \in \mathbf{Z}$) be the positions of the (hyper-) atoms of the decoration with respect to the unit cell of \mathcal{L} . If

$$\rho_0(\mathbf{r}) = \sum_{i=1}^k \rho_i(\mathbf{r}) * \delta(\mathbf{r} - \mathbf{r}_i), \quad (21)$$

where $\rho_k(\mathbf{r})$ refers to a single hyperatom, then

$$\hat{\rho}_0(\mathbf{u}) = \sum_{i=1}^k \hat{\rho}_i(\mathbf{u}) \exp(-2\pi i \mathbf{u} \cdot \mathbf{r}_i). \quad (22)$$

For $\rho_i(\mathbf{r})$ we propose the form

$$\rho_i(\mathbf{r}) = \rho_i^3(\mathbf{r}'') * \delta(\mathbf{r}^\perp), \quad (23)$$

where $\rho_i^3(\mathbf{r}'')$ is the density of an ordinary three-dimensional atom (from now on it will be assumed that $E'' = \mathbf{R}^3$). Consequently,

$$\hat{\rho}_i(\mathbf{u}) = \rho_i^3(\mathbf{u}'') \quad (24)$$

and

$$\hat{\rho}_0(\mathbf{u}) = \sum_{i=1}^k \hat{\rho}_i^3(\mathbf{u}'') \exp(-2\pi i \mathbf{u} \cdot \mathbf{r}_i). \quad (25)$$

Putting everything together we find that

(1) If W does not depend on \mathbf{r}'' then \hat{W} is a δ function and the pattern consists of strict δ functions. This corresponds to a perfect quasicrystal (quasiperiodic).

(2) If the up-and-down jumps of the band are themselves quasiperiodic, with wave vectors that are also wave vectors of the corresponding perfect quasicrystal, then the diffraction pattern will consist again of δ functions.

(3) If the jumps are random, the pattern will consist of Bragg peaks plus diffuse scattering.

(4) In general, the diffraction pattern consists of "peaks" centered on 1^* whose shapes are given by \hat{W} , the Fourier transform of the cut function. When W is chosen according to the needs of the DR model to produce quasicrystals (see Sec. III C) then \hat{W} will display short-wavelength components (due to the "jumps" of the band to reach the O points) but it will not display long-wavelength components (since over distances much longer than the distances between O points the band is rather flat and follows the manifold E'' closely). Consequently the diffraction pattern of the DR structures will consist of Bragg peaks plus diffuse scattering. The model can be used to build other structures where peak broadening can be expected.

The reader must be aware of a subtlety concerning Eq. (26). According to this equation the spots have a shape governed by the transform of W . However it may happen that different W 's (with different transforms) cut exactly the same portion of the hyperlattice and, consequently, lead to the same diffraction pattern (the authors are indebted to one of the PRB referees for pointing this out). For this reason the ups and downs of the band do not, in themselves, guarantee the presence of diffuse scattering.

V. CONCLUSIONS

The DR model provides a physical mechanism to generate structures which model crystals, multiply twinned particles, and quasicrystals. The formulation presented here clarifies several important features of the model as the long-range-order properties and the geometry of the clusters. The present results can be summarized as follows.

(1) The DR model provides a dynamical theory pathway to the final alloy, thus linking the concepts of growth and structure.

(2) The DR method can be formulated in the context of

a cut-projection scheme with a peculiar window function.

(3) The procedure to construct the strip assures that the contained hypersurface is unbroken. It leads to quasicrystals which framework is composed of tilings by rhombohedra.

(4) Although in the DR model the overlap of clusters is permitted, there exist paths for the hypersurface which recover these clusters along threefold directions, making it possible to generate cluster-based quasicrystals.

(5) In our model the higher-dimensional lattice is decorated. The resulting structure in \mathbf{R}^3 is not simply the result of decorating the tiles with a fixed motif. Rather, it could be described as a window cutting a decorated lattice in \mathbf{R}^6 permitting it to "chop out" the decoration. Other models can also be viewed as window cuts but they must either include the full decoration (ICO1-DODE-ICO2) or none at all. The resulting 3D structure thus consists of a set of identically decorated vertices.

(6) The diffraction pattern of DR structures consists, in general, of Bragg peaks plus diffuse scattering. The model can be used to model other structures where peak broadening can be expected.

(7) In spite of the fruitfulness of the higher-dimensional approach, the \mathbf{R}^3 formulation of the DR model has some distinctive advantages such as providing a physically and geometrically clear easy way of producing arbitrary De-launay systems,³² periodic or not.

ACKNOWLEDGMENTS

The authors wish to thank Alan I. Goldman and Manuel Torres for helpful ideas and comments. Technical support, from C. Zorrilla and L. Beltrán del Rio and photographic aid by A. Sánchez is acknowledged. This work was financially supported by CONACYT, through Grant No. P228CCOX-891641, and DGAPA (UNAM) through Grant No. IN-104989. D. Romeu wishes to express his gratitude to Professor Kamil Klier from Lehigh University for providing access to supercomputer time used in cluster calculations.

¹*Proceedings of the Workshop on Aperiodic Crystals*, edited by D. Gratias and L. Michel [J. Phys. (Paris) Colloq. **47**, C3 (1986)].

²*The Physics of Quasicrystals*, edited by P. J. Steinhardt and S. Ostlund (World Scientific, Singapore, 1977).

³*Aperiodicity and Order I, II, and III*, edited by M. V. Jaric and D. Gratias (Academic, New York, 1988).

⁴*Proceedings of the Third International Meeting on Quasicrystals, Mexico, 1989*, edited by M. José-Yacamán, D. Romeu, V. Castaño, and A. Gómez (World Scientific, Singapore, 1990).

⁵D. Shechtman, D. Blech, D. Gratias, and J. W. Cahn, Phys. Rev. Lett. **53**, 1951 (1984).

⁶D. Levine and P. J. Steinhardt, Phys. Rev. Lett. **53**, 2477 (1984).

⁷J. E. S. Socolar and P. J. Steinhardt, Phys. Rev. B **34**, 617 (1986).

⁸M. Audier and P. Guyot, Philos. Mag. Lett. **58**, 17 (1988).

⁹V. Elser, *Proceedings of the XVth International Colloquium on*

Group Theoretical Methods in Physics (World Scientific, Singapore, 1988), Vol. 1.

¹⁰V. Elser, *Aperiodicity and Order III*, edited by M. V. Jaric and D. Gratias (Academic, New York, 1988).

¹¹C. L. Henley, J. Phys. A **21**, 1649 (1988).

¹²K. J. Strandburg, Phys. Rev. B **40**, 6071 (1989).

¹³P. W. Stephens and A. I. Goldman, Phys. Rev. Lett. **56**, 1168; **57**, 2331 (1986).

¹⁴P. W. Stephens, *Aperiodicity and Order III*, edited by M. V. Jaric and D. Gratias (Academic, New York, 1988).

¹⁵D. Romeu, Int. J. Mod. Phys. B **2**, 265 (1988).

¹⁶D. Romeu, Int. J. Mod. Phys. B **2**, 77 (1988).

¹⁷D. Romeu, Acta Metall. Mater. **38**, 113 (1990).

¹⁸D. Romeu (unpublished).

¹⁹C. L. Henley, Phys. Rev. B **43**, 993 (1991).

²⁰C. L. Henley, Commun. Condens. Matter Phys. **13**, 59 (1987).

²¹A. L. Mackay, Kristallografiya **26**, 910 (1981) [Sov. Phys. Crystallogr. **26**, 517 (1981)].

- ²²P. Kramer and R. Neri, *Acta Crystallogr. A* **40**, 580 (1984).
- ²³A. Gómez, J. L. Aragón, and F. Dávila, *J. Phys. A* **24**, 493 (1991).
- ²⁴M. Duneau and A. Katz, *Phys. Rev. Lett.* **54**, 2688 (1985).
- ²⁵V. Elser, *Acta Crystallogr. A* **42**, 36 (1985).
- ²⁶P. A. Kalugin, A. Y. Kitaev, and L. S. Levitov, *Pis'ma Zh. Eksp. Teor. Fiz.* **41**, 119 (1985) [*JETP Lett.* **41**, 145 (1985)].
- ²⁷H. Terrones and D. Romeu (unpublished).
- ²⁸I. A. Harris, R. S. Kidwell, and J. A. Northby, *Phys. Rev. Lett.* **53**, 2390 (1984).
- ²⁹J. J. Saenz, J. M. Soler, and N. García, *Chem. Phys. Lett.* **114**, 15 (1985).
- ³⁰J. Farges, M. F. De Feraudi, B. Raoult, and G. Torchet, *Surf. Sci.* **156**, 370 (1985).
- ³¹S. Ranganathan, *Acta Crystallogr.* **21**, 197 (1986).
- ³²L. M. Beltrán del Rio and A. Gómez, in *Proceedings of the Third International Meeting on Quasicrystals* (Ref. 4).
- ³³J. L. Aragón, A. Gómez, and D. Romeu, *Scr. Metall. Mater.* **24**, 723 (1990).
- ³⁴A. Le Lann, *Philos. Mag.* **B 56**, 371 (1987).
- ³⁵A detailed version of this topic is planned to be published elsewhere.
- ³⁶G. Berman, J. L. T. Waugh, and L. Pauling, *Acta Crystallogr.* **10**, 254 (1957).
- ³⁷E. E. Cherkashin, P. I. Kripyakeyich, and G. I. Oleksiv, *Kristallografiya* **8**, 846 (1964) [*Sov. Phys. Crystallogr.* **8**, 681 (1964)].
- ³⁸P. Guyot and M. Audier, *Philos. Mag.* **B 52**, L15 (1985).
- ³⁹V. Elser and C. L. Henley, *Phys. Rev. Lett.* **55**, 2883 (1985).
- ⁴⁰D. Romeu, A. Gómez, and J. L. Aragón (unpublished).
- ⁴¹H. U. Nissen, R. Wessicken, C. Beeli, and A. Csanady, *Philos. Mag.* **B 57**, 587 (1987).